analyses were performed to investigate the relative importance of the factors that influence the seismic response of landfills. The discusser is concerned with the authors use of 1D analysis in lieu of more sophisticated two-dimensional (2D) analysis as "this substitution may be unsafe in many situations."

Elton et al. (1991) is a useful study, and the writers were remiss in failing to reference their work and taking advantage of its findings. In the discussion, Elton presents selected results from the 1991 paper for the case of a triangular embankment resting on bedrock. It should be noted that typical landfill geometries more closely resemble the earth dam cross sections presented in Vrymoed and Calzascia (1978) than the triangular embankment with relatively steep slopes analyzed by Elton et al. (1991), as illustrated by the typical cross sections shown in Fig. 14. Moreover, the 2D computer program used by Elton models the bedrock as a rigid boundary, hence none of the seismic energy is transmitted away from the landfill at the waste fill/foundation rock interface. Overall, however, the Elton et al. (1991) and Vrymoed and Calzascia (1978) results are similar. These studies indicate that the differences between shear stresses calculated from 1D and 2D dynamic analysis are most significant near the ground surface, especially for relatively steep slopes, but at depth (i.e. > 10 m), the 1D and 2D computed shear stresses are comparable for most cases.

In a recent evaluation of waste fill performance during the 1994 Northridge earthquake by Augello et al. (1995), the estimation of equivalent pseudostatic seismic coefficients using SHAKE91 for two waste fill cross sections (OII and Chiquita Canyon) were nearly identical to those calculated with the two-dimensional QUAD4M program (Hudson et al. 1994) for the case of base sliding. The ground below the base of the landfills was modeled in a manner analogous to that used in the paper for 1D analysis. Results for the Chiquita Canyon landfill using this program are shown in Fig. 15. It is seen that the differences between 1D and 2D analyses are, indeed, modest except for depths close to the fill surface.

For the base sliding case, which was the focus of the paper, the maximum shear stress calculated by 1D analyses is comparable to that calculated by 2D analysis for most waste fill geometries. The writers do agree with the discusser that the validity of the 1D results diminishes significantly for cases in which the cover system performance is being evaluated. In these cases, 2D analyses may be warranted. However, given the uncertainties associated with the evaluation of the dynamic properties of the waste fill, the underlying soil and bedrock properties, and the design bedrock motions, the authors judge the use of 1D analyses to be reasonable in routine design. Nevertheless, the results from 1D analyses—for that matter, also 2D analyses—should be interpreted with considerable engineering judgment, particularly when the performance of the cover system is being evaluated.

APPENDIX. REFERENCES

Augello, A. J., Matasovic, N., Bray, J. D., Kavazanjian, E. Jr., and Seed, R. B. (1995). "Evaluation of solid waste landfill performance during the Northridge earthquake." *Earthquake Des. and Perf. of Solid Waste Landfills, ASCE Geotech. Spec. Publ. No. 54, Proc. ASCE Annu. Convention*, M. K. Yegian and W. D. L. Finn, eds., ASCE, New York, N.Y., 17–50.

Hudson, M., Idriss, I. M., and Beikae, M. (1994). "QUAD4M: a computer program to evaluate the seismic response of soil structures using finite element procedures and incorporating a compliant base." Ctr. for Geotech. Modeling, Dept. of Civ. & Envir. Engrg., Univ. of California, Davis, Calif.

POLARIZATION AND CONDUCTION OF CLAY-WATER-ELECTROLYTE SYSTEMS[a]

Discussion by K. Klein[4] and J. C. Santamarina[5]

The authors measured the permittivity of two natural Leda clays (undisturbed and remoulded samples) at a frequency of 60 Hz in a capacitor-type cell. Low frequency permittivity measurements of clay-water-electrolyte systems are difficult to obtain using capacitor-type cells due to electrode polarization. This phenomenon and its implications are discussed next.

ELECTRODE POLARIZATION—ANALYSIS

The application of a low-frequency electric field produces the displacement of charges within a material. If "blocking" electrodes (e.g. platinum or gold) are used, charges accumulate against the electrodes. Thus, in the absence of electrochemical reactions, charges at the electrode form a thin capacitor which is in series with the specimen being tested. The simplest equivalent circuit for this measurement is shown in Fig. 3. The material is assumed to be nondispersive and is represented by a capacitor and a resistor in parallel: the capacitor characterizes the polarizability of the material and the resistor represents conduction losses. The total impedance Z^* of this circuit is the sum of the capacitive impedance of the polarized electrode plus the complex impedance of the material. The dependence of admittance, $Y^* = 1/Z^*$, on frequency ω is

$$Y^*_{\text{circuit}} = \frac{1}{\left(\frac{1}{R_m} + i\cdot\omega\cdot C_m\right)^{-1} - \frac{i}{\omega\cdot C_e}} \tag{14}$$

The subindices m and e refer to the material under test and the polarized electrode, respectively. Resistance R and capacitance C for parallel plate cylindrical samples can be computed as a function of sample geometry and material parameters, length d, area A, real permittivity ε', and conductivity σ

$$R = d/A\sigma; \quad C = A\varepsilon'/d \tag{2a,b}$$

Substituting (2*a*) and (2*b*) into (1)

$$Y^*_{\text{circuit}} = 1\Big/\left[\left(\frac{A\sigma_m}{d_m} + i\omega\frac{A\varepsilon'_m}{d_m}\right)^{-1} - \frac{id_e}{\omega A\varepsilon_0}\right] \tag{3}$$

where the permittivity of the polarized electrode is assumed to be equal to $\varepsilon_0 = 8.85\cdot 10^{-12}\ C^2/J\cdot m$ which is the permittivity of free space. The complex admittance of a capacitor as a function of the complex permittivity of the material is

$$Y^*_{\text{capacitor}} = (\kappa'' + i\cdot\kappa')\omega(A\cdot\varepsilon_0/d) \tag{4}$$

where κ' and κ'' are the real and imaginary relative permittivities ($\kappa^* = \varepsilon^*/\varepsilon_0$). Equating the admittance of a true capacitor, (4) with the admittance of the circuit, (3), and solving for the real and imaginary permittivities (assuming $d_m >> d_e$):

$$\kappa' = \frac{\text{Im}(Y^*_{\text{circuit}})d_m}{\omega\varepsilon_0 A} = \frac{\left(\frac{\sigma_m}{\varepsilon_0\cdot\omega}\right)^2\frac{d_e}{d_m} + \kappa'_m}{1 + \left(\frac{d_e}{d_m}\right)^2\left(\frac{\sigma_m}{\varepsilon_0\cdot\omega}\right)^2} \tag{5}$$

[a]March 1995, Vol. 121, No. 3, by J. Q. Shang, K. Y. Lo, and I. I. Inculet (Paper 7559).

[4]Grad. Student, Univ. of Waterloo, Waterloo, Ontario N2L 3G1, Canada.

[5]Assoc. Prof., Univ. of Waterloo, Waterloo, Ontario, Canada.

$$\kappa'' = \frac{\mathrm{Re}(Y^*_{\text{circuit}})d_m}{\omega\varepsilon_0 A} = \frac{\sigma_m/\varepsilon_0\omega}{1 + (d_e/d_m)^2(\sigma_m/\varepsilon_0\omega)^2} \quad (6)$$

These equations define the spectral values for κ^* that would be measured for a homogeneous material with constant permittivity, when the measurement is affected by electrode polarization. The lower and upper bounds for the measured real permittivity are

$$\kappa' = \kappa'_m \quad \text{(high frequencies)} \quad (7)$$

$$\kappa' = d_m/d_e \quad \text{(low frequencies)} \quad (8)$$

Hence, the permittivity κ' measured at high frequencies has no electrode effects. However, low frequency measurements may bear no relation to the permittivity of the medium κ'_m.

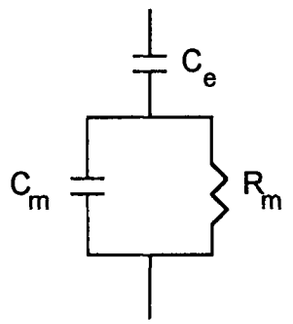

FIG. 3. Equivalent Circuit of a Measurement with Electrode Polarization, C_e. The (Material is Represented by C_m and R_m)

TABLE 3. Characteristics of Tested Electrolytes

Sample (1)	Conductivity[a] σ_{meas} [S/m] (2)	Total dissolved solids[a] TDS_{meas} [mg/l] (3)	Estimated conductivity[b] σ_{est} [S/m] (4)	Approximated conductivity[c] σ_{approx} [S/m] (5)
Deionized water	$2.23 \cdot 10^{-3}$	11.1	$1.665 \cdot 10^{-3}$	$2.19 \cdot 10^{-3}$
NaCl	$24.7 \cdot 10^{-3}$	123	$18.45 \cdot 10^{-3}$	$21.9 \cdot 10^{-3}$
Tap water	$111 \cdot 10^{-3}$	554	$83.1 \cdot 10^{-3}$	$91.2 \cdot 10^{-3}$

[a]Measured with a conductivity-TDS meter (HACH 44600).
[b]Estimated as: $\sigma_{est} = 0.15 \cdot 10^{-3} \cdot TDS$, where σ_{est} is in S/m and TDS is in mg/L.
[c]Approximated from the slope of log(ε″)—log(ω) graph—Eq. (9).

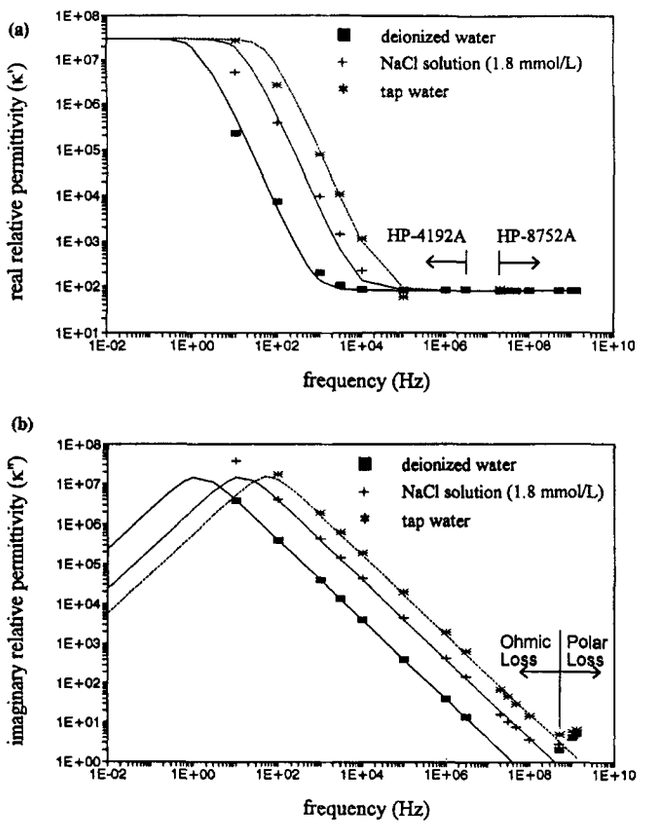

FIG. 4. Complex Permittivity of Selected Electrolytes (Electrode Polarization is Clearly Seen in κ' at Frequencies below $f \approx 10^4$ Hz)

larization. The lower and upper bounds for the measured real permittivity are

Experimental Study

The permittivities of three aqueous electrolytes (commercial deionized water, a 1.8 mmol/L NaCl solution, and tap water) were measured in a cylindrical capacitor cell with an impedance analyzer (HP-4192A, 10 Hz to 13 MHz). For completeness, high frequency measurements were conducted with an impedance analyzer and a coaxial termination probe (HP-8752A and HP-85070A, 20 MHz to 1.3 GHz). The characteristics of these electrolytes are presented in Table 3. The real and imaginary permittivities, computed without correcting for electrode polarization, are shown in Fig. 4. Continuous lines correspond to Equations 5 and 6.

The decrease in imaginary permittivity (κ'') with frequency is governed by the dc conductivity of the material σ_m, as can be seen from Equation 6,

$$\kappa''_{dc} \cong \sigma_m/\omega\varepsilon_0 \quad (9)$$

At high frequencies ($f > \approx 10^9$ Hz), molecular orientation polarization losses begin to manifest, producing the observed increase in κ''. The corresponding decay in κ' due to the orientational relaxation of free water cannot be seen on this log scale.

The real permittivity (κ') computed without correcting for electrode polarization is high at low frequencies, reaching the upper bound $\kappa' = d_m/d_e$, and decreases with increasing frequency until the constant value κ'_m is obtained. The high κ' values at low frequencies are governed by electrode polarization since there is no additional polarization mechanism acting at these frequencies. The frequency ω_{break} where κ' reaches κ'_m increases with the conductivity of the material σ_m; it was approximately 10^4 Hz, 10^5 Hz, and 10^6 Hz for deionized water, NaCl solution, and tap water, respectively. For frequencies $\omega < \omega_{break}$, the measured κ' is directly affected by the conductivity of the material σ_m and it is almost independent of the true permittivity of the material κ'_m. The thickness of the equivalent capacitor d_e representing the polarized electrode was determined by fitting the simple equivalent circuit shown in Fig. 3 to measured values. The thickness was found to be $d_e \approx 10^{-9}$ m for all samples, which is in the order of molecular size.

It is very difficult to remove electrode polarization effects because errors between measured and modeled values are of the same order of magnitude as the measurement, thus, an exponentially dependent error must be subtracted on a linear scale. Alternatives have been proposed to enhance the measurement of ε^* at low frequencies with capacitor probes (e.g. include air or teflon gap, measure samples of two thicknesses and subtract to cancel electrode effects, use electrochemically reversible electrodes). However, all these methods lead to highly uncertain results. Electrode polarization effects can be minimized through the use of a four-terminal system (e.g. Olhoeft 1981).

APPENDIX. REFERENCE

Olhoeft, G. R. (1981). *Physical properties of rocks and minerals*, Vol. II-2, McGraw-Hill/CINDAS Data Series on Material Properties, McGraw-Hill Book Co., Toronto, Canada, 257–329.